The non-enzymatic RAS effector RASSF7 inhibits oncogenic c-Myc function

Anbarasu Kumaraswamy[1], Anitha Mamidi[1], Pavitra Desai[1], Ananthi Sivagnanam[1] Lakshmi Revathi Perumalsamy[1], Chandrasekaran Ramakrishnan[2], Michael Gromiha[2], Krishnaraj Rajalingam[3] and Sundarasamy Mahalingam[1*]

[1]National Cancer Tissue Biobank, Laboratory of Molecular Cell Biology, [2]Protein Bioinformatics Laboratory, Bhupat and Jyoti Mehta School of Biosciences, Department of Biotechnology, Indian Institute of Technology-Madras, Chennai, India;
[3]MSU-FZI, Institute of Immunology, University Medical Center Mainz, JGU, Mainz, Germany

Running Title: *RASSF7 regulates c-Myc function*

*To whom correspondence should be addressed: Sundarasamy Mahalingam, Laboratory of Molecular Cell Biology, Room No: 403, Department of Biotechnology, Indian Institute of Technology-Madras, Chennai 600036, India; mahalingam@iitm.ac.in; Tel: (+91-44) 22574130; FAX: (+91-44) 22574102.

Keywords: RASSF7, c-Myc, Ubiquitination, Tumorigenesis, Cell Penetrating Peptide, Peptide Inhibitor, Cell Proliferation, Cancer, MAX, Transcription Factor

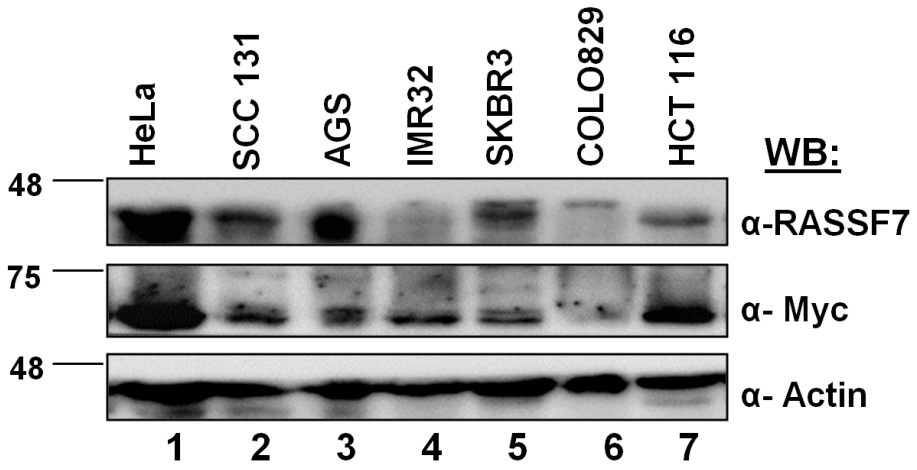

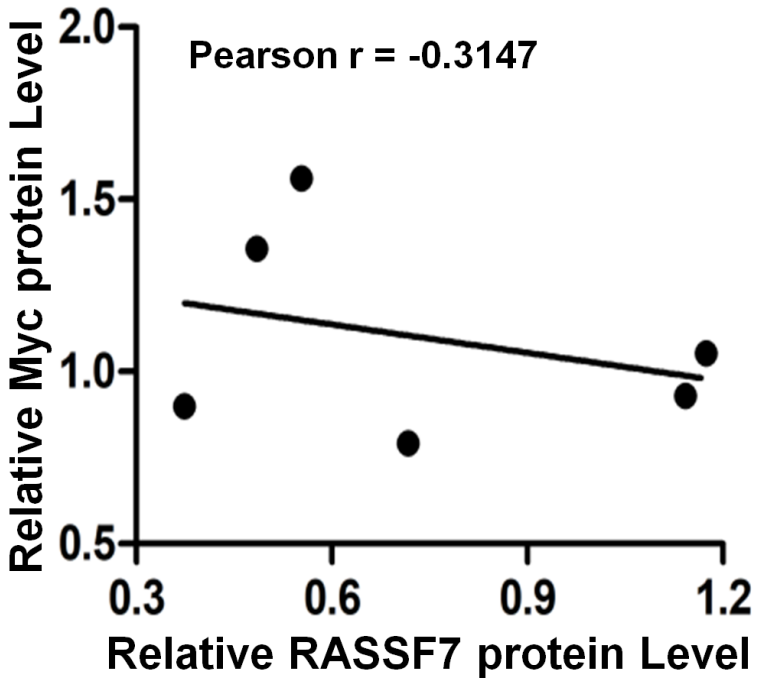

Figure: S1

Western blot analysis in cancer cell lines reveals the existence of inverse correlation between RASSF7 and c-Myc protein levels. Densitometry analysis was performed for RASSF7 and Myc protein levels normalized to Actin.

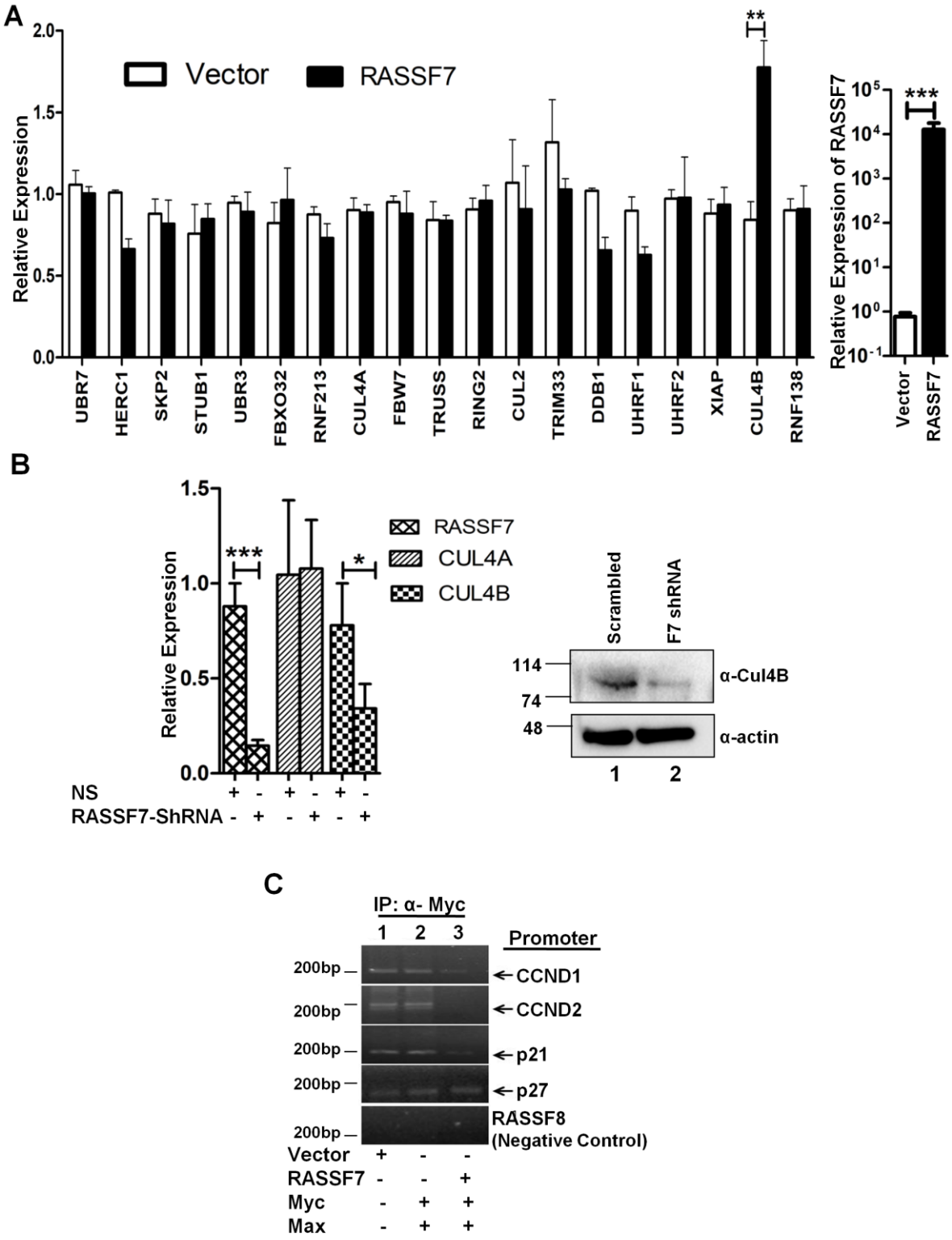

Figure: S2

(A) RT-qPCR analysis of different E3 ligases expression in presence of RASSF7 in HEK293T indicates that Cullin4B (CUL4B) was significantly upregulated. Beta-actin served as internal control. **(B)** RT-qPCR and western blot analyses indicate that depletion of RASSF7 reduces endogenous CUL4B expression levels. Beta-actin served as internal control (n=3 and data is expressed as mean±SD). **(C)** Chromatin immunoprecipitation assay reveals that RASSF7 alters c-Myc occupancy on target promoters. RASSF8 promoter lacking c-Myc binding site served as negative control.

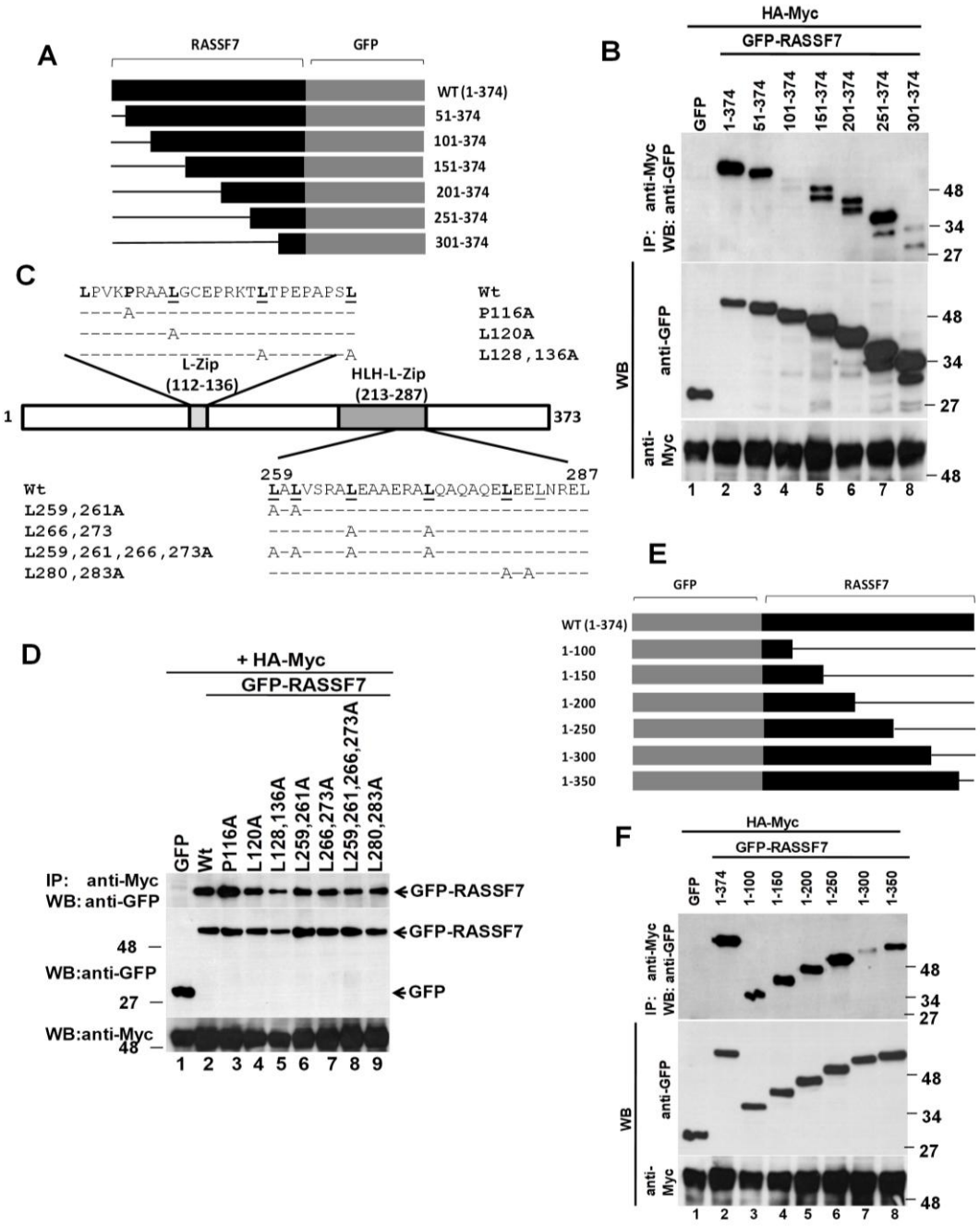

Figure: S3

(A) Schematic diagram indicating the wild-type and N-terminal deletion mutants of RASSF7. **(B)** Various indicated N-terminal deletion mutants of RASSF7 were expressed in HEK293T cells and performed immunoprecipitation assay using anti-c-Myc antibodies. Results indicate that all RASSF7 mutants are interacting with c-Myc. **(C)** Schematic representation L-Zip and HLH-L-Zip domains mutants of RASSF7. All underlined amino acids were mutated with alanine as described in Materials and Methods. **(D)** Immunoprecipitation analysis with HEK293T cell lysates indicated that all L-Zip and HLH-L-Zip domains mutants of RASSF7 are able to interact with c-Myc. **(E)** Line diagram indicating the wild-type and C-terminal deletion mutants of RASSF7. **(F)** All indicated C-terminal deletion mutants of RASSF7 were expressed in HEK293T cells and performed immunoprecipitation assay using anti-c-Myc antibodies. Results indicate that all RASSF7 mutants are interacting with c-Myc.

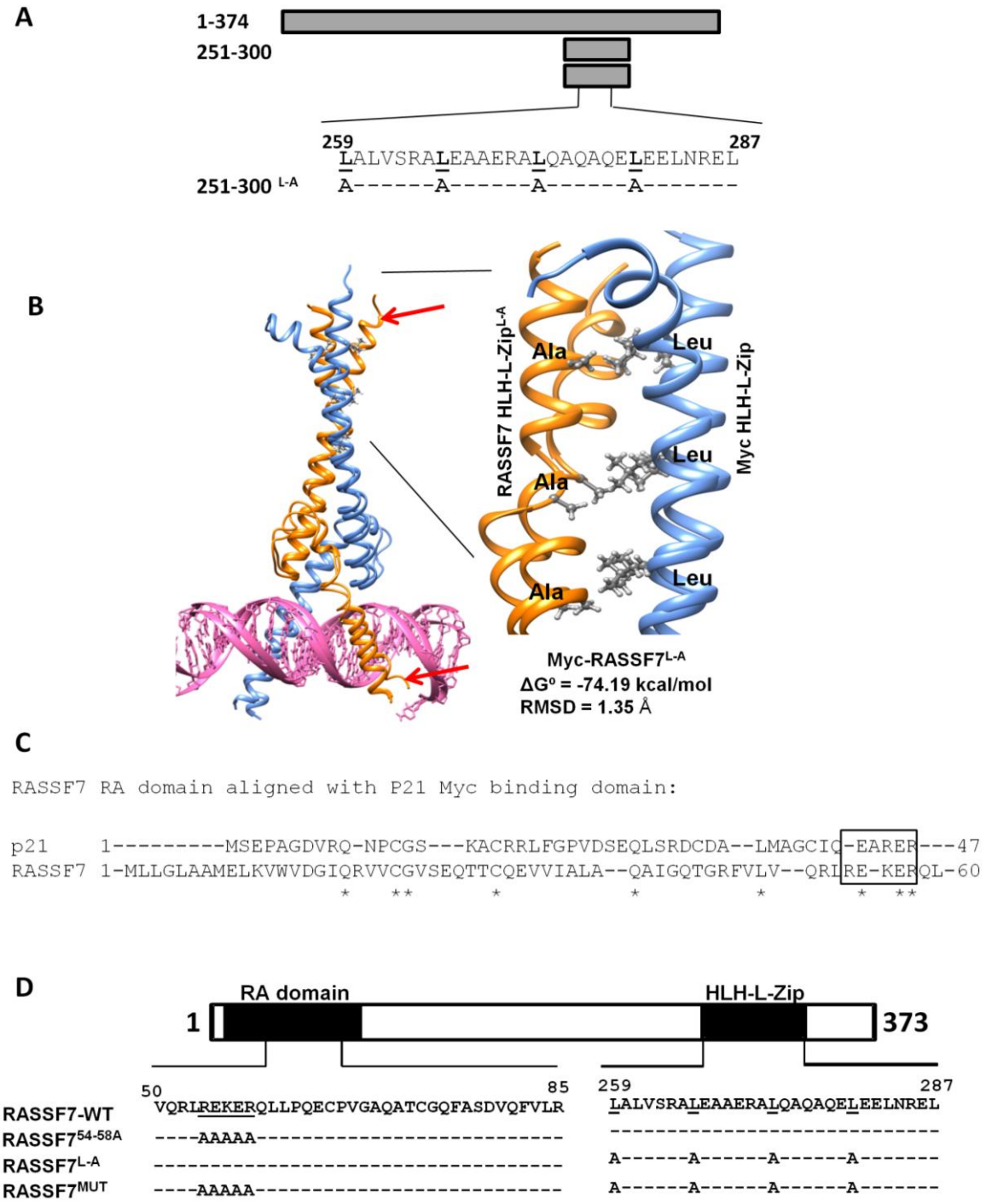

Figure: S4

(A) Schematic representation of HLH-L-Zip domain mutants of RASSF7. All underlined amino acids were mutated with alanine as described in Materials and Methods. **(B)** Snapshot of c-Myc-RASSF7^{L-A} heteromeric complex shows reduced stability (indicated by arrows). The lack of interaction between mutated alanine (RASSF7 chain) and leucine (c-Myc chain) are showed as magnified image. **(C)** Alignment of amino acid sequences from p21 domain interacting with c-Myc with RA domain of RASSF7 indicating a conservation between these domains (indicated in box). **(D)** Schematic line diagram of RASSF7 containing mutations RA domain and HLH-L-Zip domain. All underlined amino acids were mutated with alanine as described in Materials and Methods.

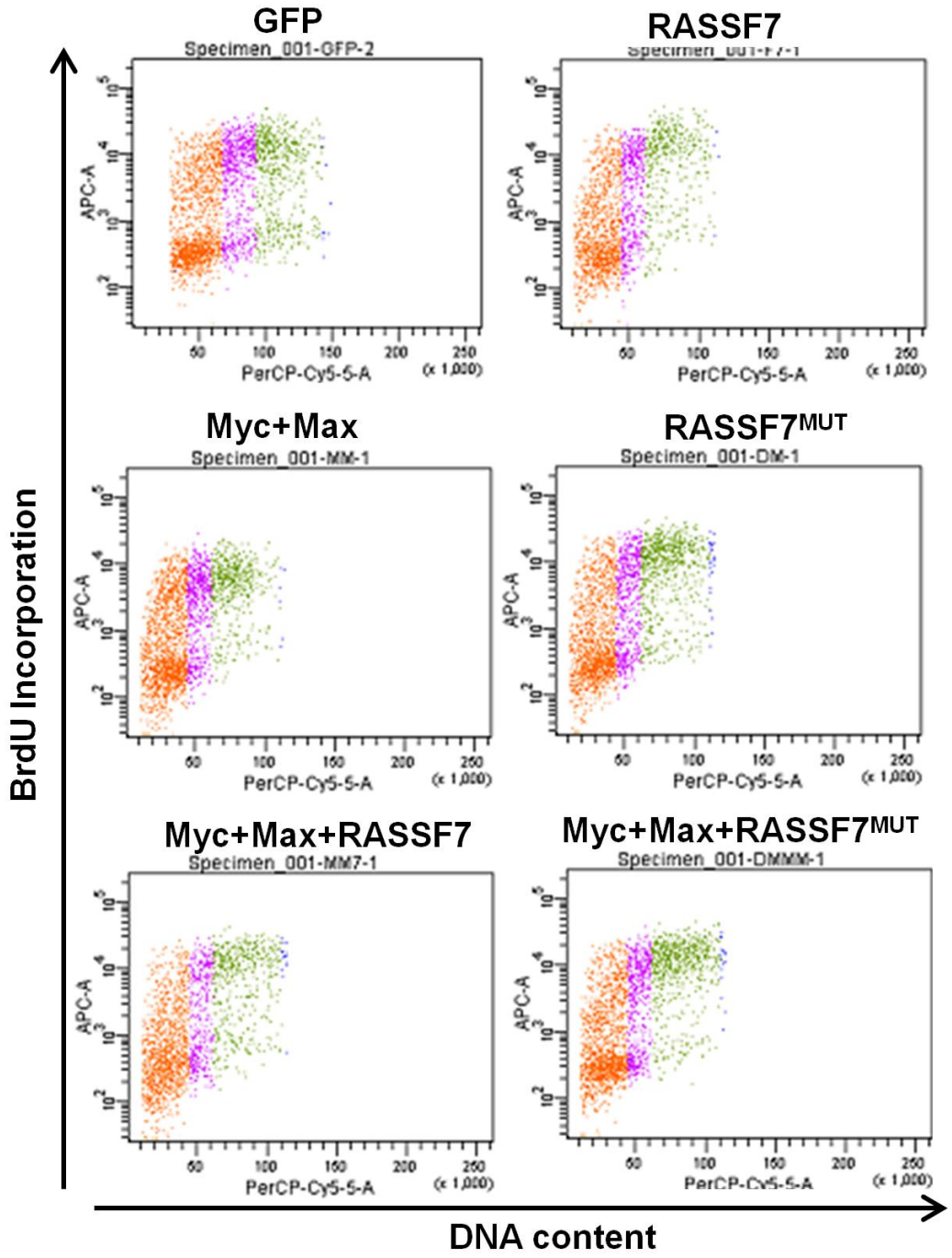

Figure: S5

Representative BrdU assay bivariate plots of HEK293T cells upon co-expression of wild-type RASSF7 or c-Myc interaction deficient mutant of RASSF7 (RASSF7^{MUT}) with c-Myc and Max. The DNA stained with 7-AAD is represented in X-axis and BrdU incorporation in Y-axis.

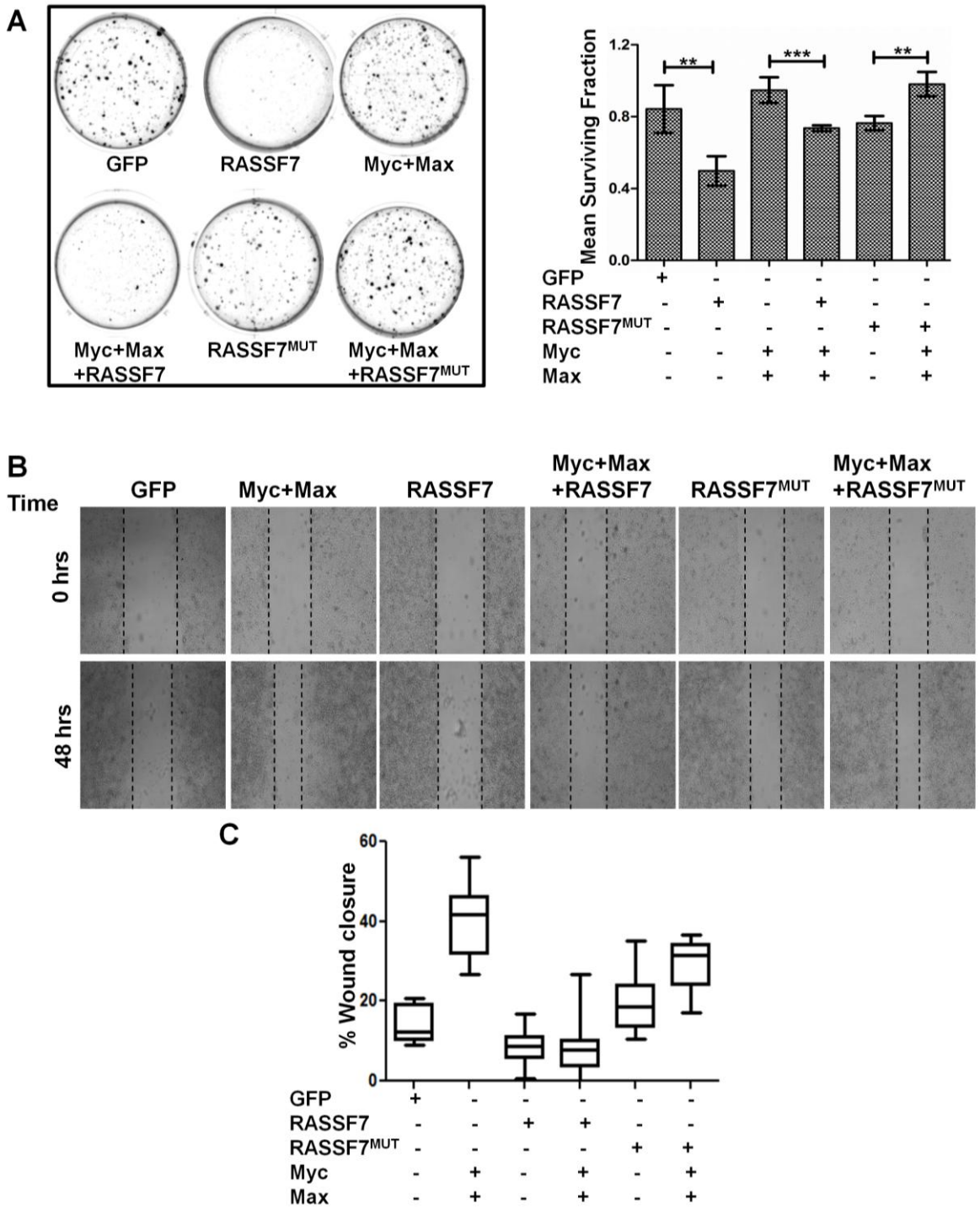

Figure: S6

(A) Representative Images of colony forming assay performed in HeLa cells indicated that c-Myc induced colony forming ability was inhibited by RASSf7^{WT} but not RASSF7^{MUT}. Colonies were counted using ImageJ and surviving fraction was calculated and plotted as bar diagram. (n=3 and data is expressed as mean ± SD). **(B)** HeLa cells were transiently expressed with indicated proteins and performed wound healing assay. Results indicate that c-Myc induced cell migration was inhibited by RASSf7^{WT} but not RASSF7^{MUT}. **(C)** Wound areas from the wound healing assay were analysed and %wound closure after 48 hours was calculated and plotted as box plots. (n=3 and data is expressed as mean ± SD).

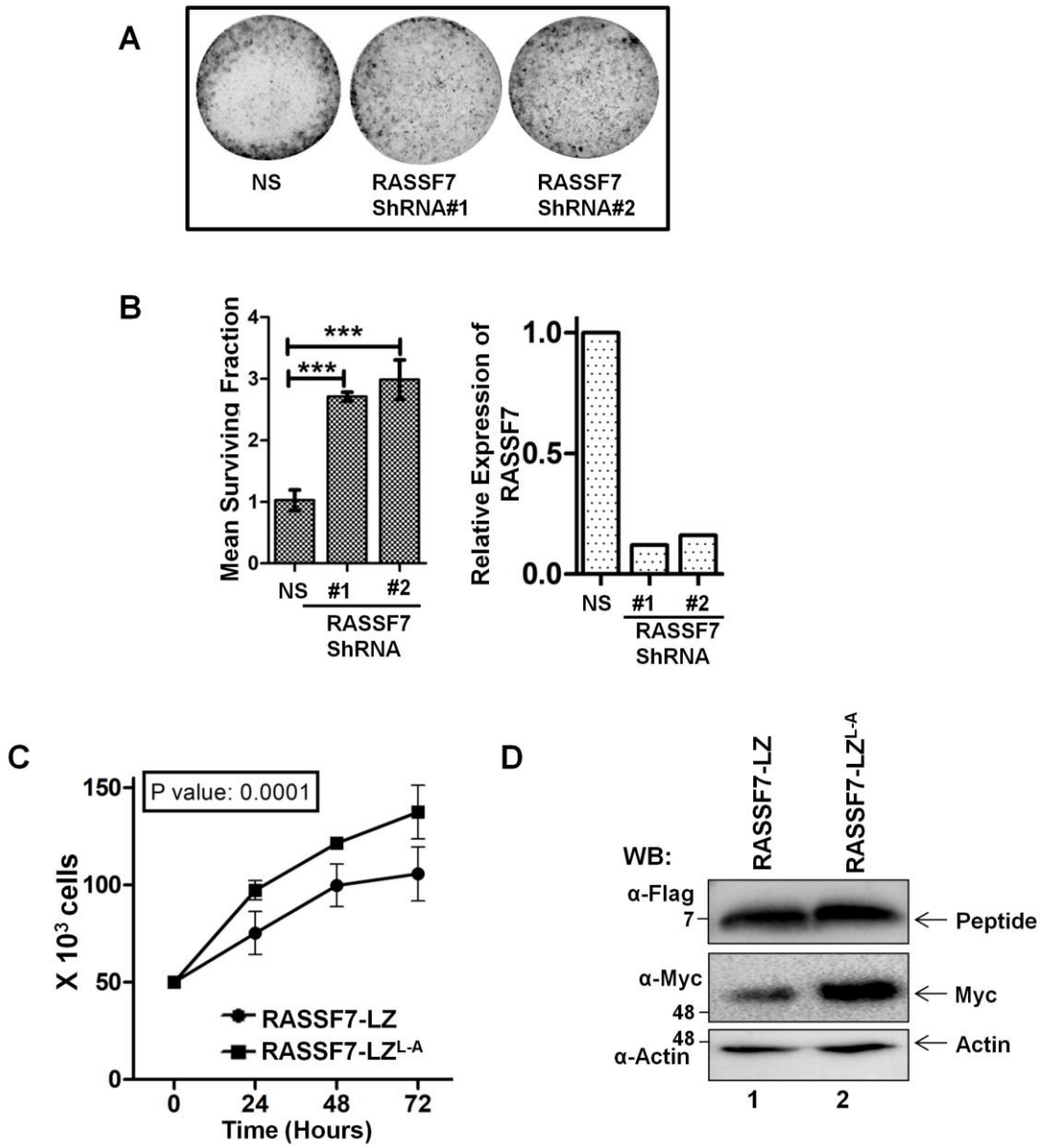

Figure: S7

(A) Immortalized NIH3T3 cells were transfected with RASSF7 shRNA plasmids and colony forming assay was performed. Results indicate that depletion of RASSF7 increased number of colonies. **(B)** Colonies from RASSF7 depleted NIH3T3 cells were counted using ImageJ and surviving fraction was calculated and plotted as bar diagram. (n=3 and data is expressed as mean ± SD). Knockdown of RASSF7 was confirmed by RT-qPCR. Beta-actin served as internal control. **(C)** HEK293T cells showed decreased proliferation upon treatment with RASSF7-LZ peptide as revealed by cell counting performed at indicated time intervals. **(D)** Treatment of RASSF7-LZ peptide induces reduction in endogenous c-Myc levels in HEK293T cells.